

## Surface growth on diluted lattices by a restricted solid-on-solid model

Changhan Lee and Sang Bub Lee\*

*Department of Physics, Kyungpook National University, Daegu 702-701, Republic of Korea*

(Received 5 May 2009; published 28 August 2009)

An influence of diluted sites on surface growth has been investigated, using the restricted solid-on-solid model. It was found that, with respect to equilibrium growth, the surface width and the saturated width exhibited universal power-law behaviors, i.e.,  $W \sim t^\beta$  and  $W_{\text{sat}} \sim L^\zeta$ , regarding all cases with respect to the concentration of diluted sites  $x=1-p$ , with  $p$  being the occupation probability on each lattice site. For  $x < x_c$  ( $=1-p_c$ ,  $p_c$  being the percolation threshold), the growth appeared to be similar to that of a regular lattice, both in two and three dimensions. For  $x=x_c$ , the growth yielded nontrivial exponents which were different from those on a regular lattice. In nonequilibrium growth, a considerable amount of diluted sites ( $x \leq x_c$ ) appeared to yield nonuniversal growth, unlike the case of a regular lattice. The cause of nonuniversal growth dynamics has been investigated, considering the growth on a backbone cluster and on lattices constructed with periodically and randomly diluted subcells.

DOI: [10.1103/PhysRevE.80.021134](https://doi.org/10.1103/PhysRevE.80.021134)

PACS number(s): 05.20.-y, 64.60.Ht, 68.35.Ct, 05.70.Np

### I. INTRODUCTION

Over the last several decades, surface roughening has been extensively studied by using various continuum growth equations as well as discrete atomistic models [1,2]. Surface roughening is associated with a wide variety of other systems, such as domain walls in regards to the two-dimensional random bond Ising model [3], randomly stirred fluids [4], ballistic aggregation [5], and directed polymers in a random potential [6,7].

The most well-known continuum equation describing the surface growth is the Kardar-Parisi-Zhang (KPZ) equation, given as [8]

$$\frac{\partial h}{\partial t} = \nu \nabla^2 h + \frac{\lambda}{2} (\nabla h)^2 + \eta(\vec{r}, t), \quad (1)$$

where  $\eta$  represents the Gaussian random variable that satisfies

$$\langle \eta(\vec{r}, t) \eta(\vec{r}', t') \rangle = 2\Gamma \delta(\vec{r} - \vec{r}') \delta(t - t'), \quad (2)$$

with  $\Gamma$  describing the local noise variation. Various discrete models which are very different from each other, such as the Eden model [9], the ballistic deposition [10], and the restricted solid-on-solid (RSOS) model [11], are all known to be described by the KPZ equation, and these models are considered to belong to the KPZ universality class. There are other known universality classes, such as the Edwards-Wilkinson class [12] as well as the Herring-Mullins class [13], all of which were studied on a pure substrate.

Since the surface structure of many growth processes is self-affine, most efforts were concentrated on measuring the height fluctuations. The surface width,  $W$ , is defined as the standard deviation, or the root-mean-square fluctuation of heights,

$$W(t, L) = \langle [h(\vec{r}, t) - \overline{h(t)}]^2 \rangle^{1/2}, \quad (3)$$

where  $h(\vec{r}, t)$  represents the local height variable at the site  $\vec{r}$  and time  $t$ ,  $\overline{h(t)}$  represents the average height over lattice sites, and  $\langle \dots \rangle$  denotes the average over various samples. Here,  $d$  is the substrate dimension and, therefore, the total dimension is  $d+1$ . It is generally hypothesized that  $W(t, L)$  obeys the scaling relation, given as [14]

$$\begin{aligned} W(t, L) &\sim L^\zeta f(t/L^z) \rightarrow t^\beta, & t \ll L^z, \\ &\rightarrow L^\zeta, & t \gg L^z, \end{aligned} \quad (4)$$

where the scaling function  $f(x)$  is  $x^\beta$  for  $x \ll 1$  and is constant for  $x \gg 1$ . The roughness exponent  $\zeta$  is the quantity that describes the characteristic of the saturated surface width at a sufficiently late time. The exponents  $\beta$  and  $z$  are associated with each other by the relationship  $z\beta = \zeta$ . In the equilibrium growth, with the same probabilities regarding deposition and evaporation, the nonlinear term vanishes with  $\lambda=0$ . Equation (1), thus, becomes the Edwards-Wilkinson equation, which can be solved exactly, yielding  $\beta=(2-d)/4$ ,  $\zeta=(2-d)/2$ , and  $z=2$ . In the nonequilibrium growth with  $\lambda \neq 0$ , the KPZ equation is solved exactly only in one dimension, with  $\beta=\frac{1}{3}$  and  $\zeta=\frac{1}{2}$ . In 2+1 dimensions, the exponents were obtained by means of numerical simulations as  $\zeta=0.38 \sim 0.40$  and  $\beta=0.24 \sim 0.25$  [7,11,15–17].

In regards to the growth on a substrate with a quenched noise and a driving force, the exponents were found to be different from those on a regular lattice [18–22]. This problem was introduced in order to elucidate different physical situations, such as the driven interface of moving fluids through pores of random geometry. This type of disorder is known to lead to interface pinning at a sufficiently small driving force, and the roughness exponent is larger in comparison to the growth on a pure substrate. As the driving force increases, the pinning-depinning transition occurs at a critical point, at which the pressure value of the moving fluid is associated with the critical density of the directed percolation. Above the critical point, the growth exponent  $\beta$  recovers to the value of the KPZ universality.

\*Corresponding author; [sblee@knu.ac.kr](mailto:sblee@knu.ac.kr)

Surface roughening by RSOS model was also studied on various geometrical fractal substrates in order to understand how the intrinsic properties of the substrates influence the critical exponents [23–25]. A significant progress has been achieved in understanding the growth on the fractal substrates. For example, the growth and roughness exponents with respect to the equilibrium RSOS growth were found to be represented in terms of the spectral dimension, as well as the fractal dimension, although nonequilibrium growth has not yet been fully understood. The growth and roughness exponents regarding the EW model were obtained by Zumofen *et al.* with respect to the behavior of the autocorrelation function of the associated diffusion problem [26] and, more recently by Lee and Kim, by means of a simple power-counting analysis of the fractional Langevin equation describing the surface growth on a fractal substrate [27]. The numerical data were found to confirm the analytical predictions for the growth on various geometrical fractal substrates.

Along these lines, it is natural to study the surface roughening on randomly diluted lattices or, equivalently, on a percolation cluster. The study of this problem attracts interest in two respects: first, whether or not the role of the diluted site is effectively the same as the sites with a quenched noise. Considering that the lattice dilution is simply an absence of lattice sites, it is expected that the surface grows faster, in comparison to the growth on a regular lattice, because the RSOS condition will be examined for the less number of nearest-neighbor sites. It is interesting to study as to how this reflects on the growth and roughness exponents. Second, the influence of a quenched disorder is a long standing problem in the critical phenomena. The quenched disorder, in this sense, is the lattice dilution and, therefore, an infinite percolation cluster is considered to be the lattice with a quenched disorder. Examples of such problems include the self-avoiding walks (SAWs) on randomly diluted lattices [28–30] as well as the contact process with a quenched disorder [31,32]. These problems were motivated based on the Harris criterion [33], which implies that, in regards to the magnetic system, the pure fixed point is unstable if the specific heat exponent  $\alpha$  is positive. Since the problem of SAWs is equivalent to the  $n$ -vector model in the limit of  $n \rightarrow 0$  [28,34], any small amount of impurities is expected to influence the critical behavior of SAWs if  $\alpha > 0$ . The specific heat is undefined for the SAWs; however, the exponent can be obtained from the hyperscaling relation as  $\alpha = 2 - d\nu$  [34],  $d$  and  $\nu$  representing, respectively, the lattice dimensionality and the correlation length exponent, and is indeed positive for  $d < 4$ . Similarly, with respect to the epidemic spreading, i.e., to the contact process,  $\alpha$  is positive for  $d < 4$ . In the latter case, the lattice dilution were found to yield the Griffith phase, in which the nonuniversal power-law behavior of the density of active particles was observed [31,32]. Thus, it is interesting to investigate how the diluted sites influence the surface growth as well.

In this paper, the surface growth is investigated for the equilibrium and nonequilibrium RSOS models on randomly diluted lattices of a concentration of diluted sites  $x$  ( $=1-p$ ,  $p$  being the occupation probability), i.e., on an infinite cluster of occupied sites adjacent to and above the percolation threshold  $p_c$  ( $=1-x_c$ ). The percolation cluster at  $p_c$  is known

to be fractal, with the fractal dimension of  $d_f = \frac{91}{48}$  in two dimensions (2D) [35,36] and  $d_f \approx 2.53$  in three dimensions (3D) [37]. However, for  $x < x_c$  ( $p > p_c$ ), it is known to be Euclidean. The surface growth at  $x_c$  as well as the selected values of  $x < x_c$  are particularly investigated in both 2D and 3D, in order to determine if the diluted sites influence the critical exponents. The results of this study for the equilibrium RSOS growth will enable the researchers to examine the validity of the analytical prediction for equilibrium growth on random fractal lattices.

The remainder of the paper is organized as follows. In Sec. II, the RSOS model as well as the numerical method for generation of an “incipient” infinite cluster of undiluted sites are described. In Secs. III and IV, the results with respect to the equilibrium and nonequilibrium growth are presented, in conjunction with relevant discussions and, in Sec. V, the source of nonuniversal behaviors with respect to the non-equilibrium growth is presented. The results are summarized, and the concluding remarks are presented in Sec. VI.

## II. MODELS AND METHODS

In this section, we first describe the equilibrium and non-equilibrium RSOS growth models. We then present the generation method for the percolation cluster and the averaging procedure over various samples and disorders.

### A. Restricted solid-on-solid model

The dynamic rule of the RSOS condition is to randomly select a site at  $\vec{r}$  and deposit a particle with a probability  $p_+$ , or evaporate with a probability  $p_-$ , i.e.,  $h(\vec{r}) \rightarrow h(\vec{r}) \pm 1$ , provided that the restriction regarding the local height difference

$$|\nabla h| = |h(\vec{r}) - h(\vec{r}')| \leq 1 \tag{5}$$

is satisfied between the selected site and the nearest-neighbor sites. In the equilibrium RSOS model,  $p_+ = p_- = \frac{1}{2}$  and the strength of nonlinearity vanishes, i.e.,  $\lambda = 0$ . Thus, the model is described by the EW equation. On the other hand, for  $p_+ \neq p_-$ , the growth becomes nonequilibrium in nature and the critical behavior is expected to be the same as for  $p_+ = 1$ ; i.e., the model is described by the KPZ equation.

For the growth with respect to the equilibrium RSOS model, the critical exponents were obtained by two alternative methods as [26,27]

$$\beta = \frac{1}{2} - \frac{d_s}{4} \quad \text{and} \quad \zeta = d_f \left( \frac{1}{d_s} - \frac{1}{2} \right), \tag{6}$$

where  $d_s$  represents the spectral dimension, defined by the density of normal modes on fractal lattices via  $\rho(\omega) \sim \omega^{d_s-1}$  [38], and is also related to the probability distribution of random walks returning to the origin after  $t$  steps,  $P(t) \sim t^{-d_s/2}$  [39]. Phenomenologically, the same results are obtained when considering the random deposition with correlations. In a random deposition, the surface width is known to grow in time as  $W^2 \sim t$ . In the early-time limit of the equilibrium RSOS growth, the growth is basically similar to that of the random deposition; however, as time evolves, the correlation length increases as random walks,  $\xi \sim t^{1/\zeta}$ , where  $\zeta$

represents the dynamic exponent and is equal to the dynamic exponent of random walks,  $z=z_{RW}$ , defined by the rms end-to-end distance,  $R\sim t^{1/z_{RW}}$ . Since the RSOS condition suppresses growth in the region of  $\xi^{df}$ , the surface width is assumed to be given as  $W^2(t)\propto t/\xi^{df}$ , which yields the growth exponent  $\beta$ , as illustrated in Eq. (6). Using the relations  $\zeta=\beta z$  and  $z=z_{RW}=2d_f/d_s$ , the roughness exponent is also obtained. This approach, although not scientifically confirmed, also yields the known exponents on a regular lattice.

In regards to the nonequilibrium RSOS growth, however, no successful theory other than the conjectured values based on the numerical data exists, primarily due to the nonlinear term in the KPZ equation. We, therefore, rely on the extensive numerical simulations.

### B. Generation of a percolation cluster

An infinite percolation cluster is realized as the substrate with a quenched disorder. The site percolation is employed, i.e., each of  $L^d$  lattice sites is either diluted with a probability  $x$  or occupied with a probability  $1-x$ . Any two occupied neighboring sites are assumed to be connected and to belong to the same cluster. When  $x>x_c$ , all clusters are finite, and the surface width grows linearly in time,  $W\sim t$ , on a finite cluster. When  $x\leq x_c$ , there exists an ‘‘incipient’’ infinite cluster of occupied sites which span across the lattice. The percolation cluster generated at  $x_c$ ,  $x_c\approx 0.407$  in 2D [40–42] and  $x_c\approx 0.688$  in 3D [43], is known to be fractal. However, an infinite cluster generated with respect to  $x<x_c$  is known to be Euclidean, with the substrate dimension the same as the embedding spatial dimension.

The well-known Hoshen-Kopelman algorithm [44] is employed in order to extract an infinite cluster of occupied sites. In order to proceed with growth on an infinite cluster, all the nearest-neighbor occupied sites of each lattice site are recorded to enable one to examine the local height constraint given in Eq. (5).

### C. Averaging procedure

The disorder averages of the mean-square surface width may be calculated in two different ways. In the first, a predetermined number of samples are obtained on a given disorder to calculate the sample averages and, then, the disorder averages are calculated over many different disorders. In the second, a single sample is grown on each given disorder until the surface width reaches the steady-state value, and the results are averaged over many disorders, with an equal weight over various disorders. In the SAWs problem, the averages calculated by the former method is realized as the quenched averages and the aim of this study is to calculate such averages; however, in the surface growth, the two methods would yield the same results as long as the number of samples is sufficiently large.

The main difference in averaging between the surface growth and the SAWs is the number of samples remaining up to the desired sample sizes. In the SAWs, the number of samples up to the predetermined length (steps) depends on the disorder configurations and, accordingly, the weight of each SAW depends on the disorder; therefore, the weight of

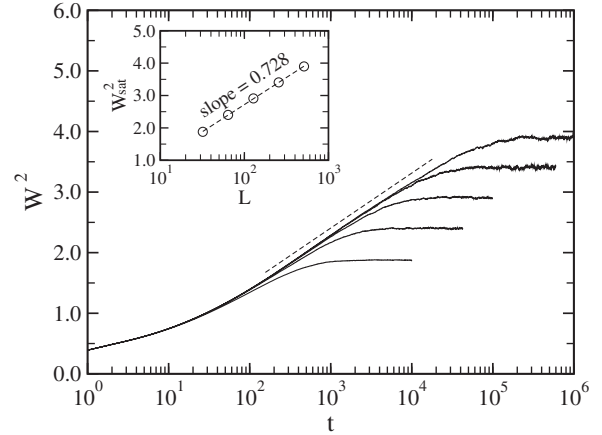


FIG. 1. The mean-square surface width  $W^2(t)$  for the equilibrium RSOS growth model on a 2D infinite percolation cluster for the concentration of diluted sites  $x=0.3$ , plotted against the evolution time  $t$  on a semilogarithmic scale. Data are for, from bottom to top,  $L=32, 64, 128, 256$ , and  $512$ . The inset shows the mean-square saturated width  $W_{\text{sat}}^2$ , calculated from the primary plotted data, plotted on a semilogarithmic scale against the size of the system.

an SAW on a disorder having less number of walks is bigger than that of the walk on a disorder having more number of walks. By this reasoning, correct averaging had been an issue for SAWs [45,46]. However, in regards to the surface growth, since all samples remain until the desired size is achieved, the weight of each sample is equal, irrespective of the disorders.

In this study, the results obtained in two different ways were compared for a particular case, i.e., for  $x=x_c$  and  $L=128$  in 2D with respect to both the equilibrium growth and nonequilibrium growth. It was found that the results averaged over 100 samples on each percolation cluster and averaged over  $3.5\times 10^3$  clusters were identical to the results averaged over  $4\times 10^3$  samples, each of which were generated on a different cluster. All presented results in this study are those obtained by the latter method.

## III. RESULTS FOR EQUILIBRIUM GROWTH

Simulations are carried out with respect to the equilibrium growth on an incipient infinite cluster generated at the selected values of  $x<x_c$ , as well as  $x_c$  in both 2D and 3D, following the RSOS growth rule.

### A. Growth on a percolation cluster above $p_c$

In order to investigate the influence of a lattice dilution on the critical exponents of surface roughening when  $x<x_c$ , simulations for  $x=0.3$  in 2D and  $x=0.6$  in 3D are carried out. The mean-square surface widths for various size systems in 2D, such as for  $L=32, 64, 128, 256$ , and  $512$ , are plotted on a semilogarithmic scale in Fig. 1. Data for various size systems yield a linear behavior before the saturations set in, except in the early stage of about 100 time steps, indicating that  $W^2\sim \ln t$ . The saturated values,  $W_{\text{sat}}^2$ , also exhibit a linear behavior on a semilogarithmic scale,  $W_{\text{sat}}^2=a+b \ln L$ , where

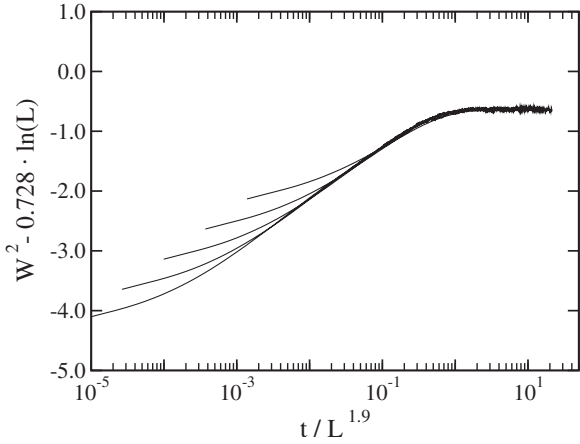


FIG. 2. The scaled mean-square surface width against the scaled time, obtained from the data in Fig. 1, plotted on a semilogarithmic scale.

$a \approx 0.63$  and  $b \approx 0.73$ , as shown in the inset. These plots clearly indicate that  $\beta = \zeta = 0$ , with logarithmic divergence, as for the growth on a regular lattice in 2D. The scaling plot of  $W^2 - b \ln L$  against  $t/L^z$  shows the best collapse for  $z = 1.9$ , as shown in Fig. 2, indicating that the dynamic exponent is also close to the known value,  $z = 2$ , on a regular lattice.

The results in 3D are presented in Fig. 3. Plotted in the main panel are the mean-square surface width against the evolution time, and those in the inset are the saturated values against the inverse size of the system. The mean-square saturated width converges to a finite value as the system size increases. This behavior is precisely the one observed on a regular lattice in 3D, indicating that  $\zeta = \beta = 0$ .

Considering the results in 2D and 3D, it is clear that the diluted sites provide a null effect on the critical exponents for the equilibrium RSOS growth, and the dynamic properties are similar to those on a regular lattice when  $x < x_c$ , implying that the pure fixed point is stable. This is generally expected

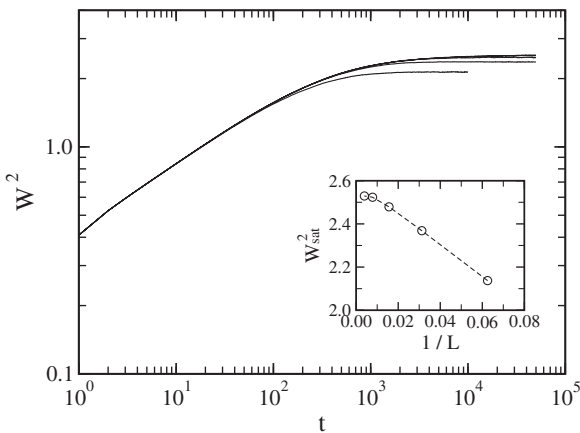


FIG. 3. The mean-square surface width  $W^2(t)$  for the equilibrium RSOS growth on a 3D infinite percolation cluster for the concentration of diluted sites  $x = 0.6$ , plotted against the evolution time  $t$  on a double logarithmic scale. Data are for, from bottom to top,  $L = 16, 32, 64, 128,$  and  $256$ . The inset shows the mean-square saturated width  $W_{\text{sat}}^2$  calculated from the primary plotted data, plotted against the inverse size of system.

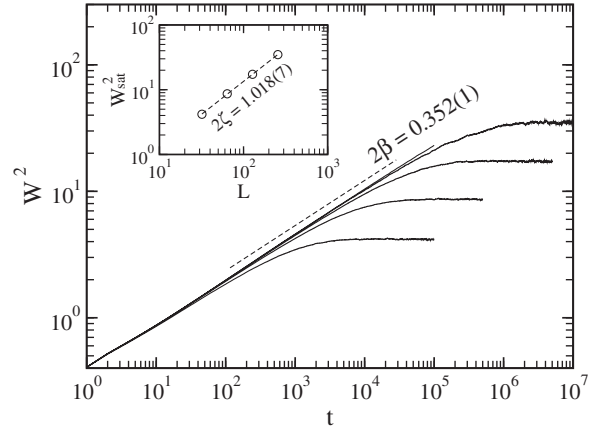


FIG. 4. The mean-square surface width  $W^2(t)$  for the equilibrium RSOS growth on a 2D infinite percolation cluster for  $x = x_c$ , plotted against the evolution time  $t$  on a double logarithmic scale. Data are, from bottom to top, for  $L = 32, 64, 128, 256,$  and  $1024$  (up to  $10^5$  time steps). The inset shows the mean-square saturated width  $W_{\text{sat}}^2$ , calculated from the primary plotted data, plotted on a double logarithmic scale against the size of the system.

because an infinite percolation cluster for  $x < x_c$  is Euclidean, although a considerable amount of lattice sites have been diluted; thus, the dynamics are expected to be similar to those on a regular lattice. However, in the nonequilibrium growth, it is not the case, as will be presented in Sec. IV.

### B. Growth on a percolation cluster at $p_c$

When the concentration of diluted sites is close to the critical value, the substrate becomes fractal, with the fractal dimension less than the spatial dimension. Thus, the growth on a fractal substrate is expected to be different from that on a regular lattice. The main panel of Fig. 4 illustrates the double-logarithmic plot of  $W^2$  generated on a 2D critical percolation network for the system sizes, from bottom to top,  $L = 32, 64, 128, 256,$  and  $1024$  (up to  $t = 10^5$ ); the inset shows the saturated values, estimated from the data in the main plot. The surface width yields a power-law behavior of  $\beta = 0.176(3)$  and  $\zeta = 0.509(7)$ . The results in 3D also yields similar characteristics, as shown in Fig. 5, with  $\beta = 0.173(3)$  and  $\zeta = 0.684(2)$ . Therefore, it is clear that the surface growth on a critical percolation cluster is different from that on a regular lattice. The results in both 2D and 3D are confirmed by the scaling analyses, as shown in Fig. 6.

The estimated values of the critical exponents are compared with the predicted values by Eq. (6). In 2D, since the spectral dimension is  $d_s \approx 1.31$  [39], the predicted values are  $\beta \approx 0.1725$ ,  $\zeta \approx 0.499$ , and  $z \approx 2.89$ . In 3D,  $d_s \approx 1.30$ , and the predictions are  $\beta \approx 0.175$ ,  $\zeta \approx 0.681$ , and  $z \approx 3.89$ . These values are in complete coincidence with the Monte Carlo data, having error margins of less than 3%.

It should be noted that the growth exponent  $\beta$  is similar to the percolation thresholds in both dimensions. This is reflected by the fact that the spectral dimension  $d_s$  is similar in both dimensions. [Note that  $\beta$  was represented in terms of  $d_s$  alone.] A number of studies had been conducted as to whether or not the spectral dimension of the percolation net-

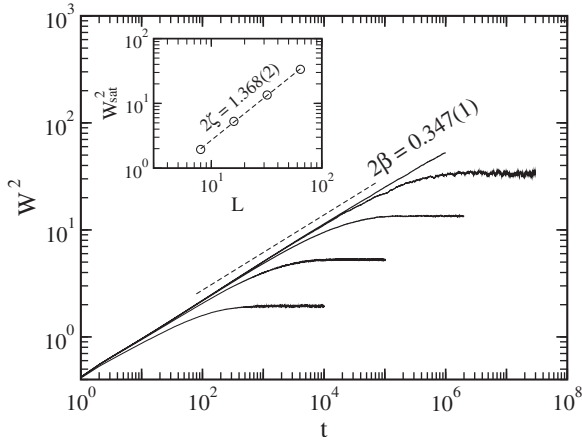


FIG. 5. The mean-square surface width  $W^2(t)$  for the equilibrium RSOS growth on a 3D infinite percolation cluster for  $x=x_c$ , plotted against the evolution time  $t$  on a double logarithmic scale. Data are for, from bottom to top,  $L=8, 16, 32, 64,$  and  $256$  (up to  $10^6$  time steps). The inset shows the mean-square saturated width  $W_{\text{sat}}^2$  calculated from the primary plotted data, plotted on a double logarithmic scale against the size of the system.

work is different with respect to different lattice dimensionality, in order to examine the Alexander-Orbach conjecture [38], in which the spectral dimension is conjectured to be  $\frac{4}{3}$  irrespective of the spatial dimensionality. Although, this conjecture was proven to be incorrect, it had been determined that the spectral dimensions were indeed close to each other.

The dynamic exponent  $z$  is close to the fractal dimension of random walks,  $d_w \approx 2.88$  in 2D and  $d_w \approx 3.88$  in 3D [47]. This is again reflected from the fact that the spatial correlation length  $\xi$  grows in time, in a similar way as the rms end-to-end distance of random walks grows in time.

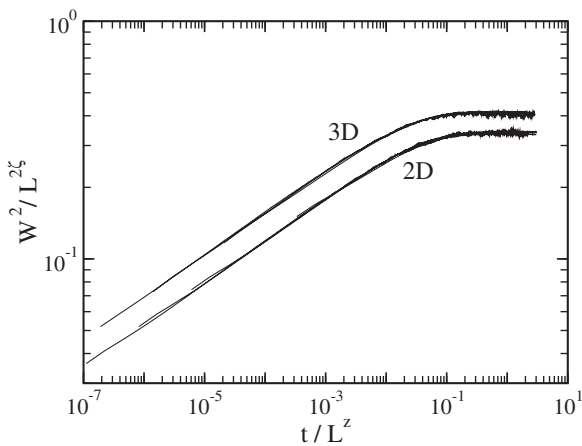


FIG. 6. The scaled mean-square surface width for the equilibrium growth on a substrate generated at  $x_c$  in 2D (bottom) and 3D (top), plotted against the scaled time. Data in 2D are scaled, using  $\zeta=0.517$  and  $z=2.888$ , as well as those in 3D using  $\zeta=0.684$  and  $z=3.886$ . Data in 3D are shifted upward by multiplying by 1.2 to avoid overlapping, and those of  $L=8$  was eliminated in the plot because they exhibited poor collapsing.

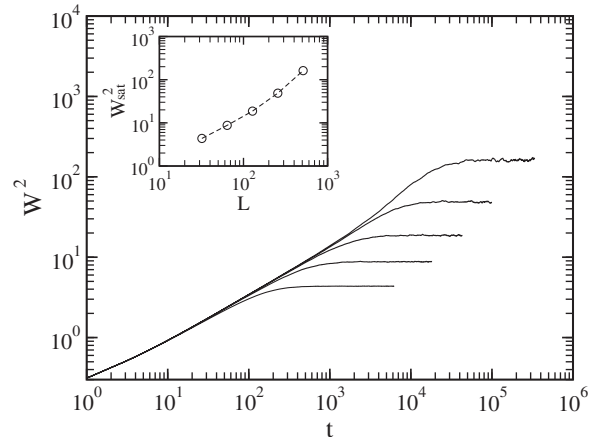


FIG. 7. The mean-square surface width  $W^2(L, t)$  for the nonequilibrium RSOS growth on a 2D infinite percolation cluster for  $x=0.35$ , plotted against the evolution time  $t$  on a double logarithmic scale. Data are for, from bottom to top,  $L=32, 64, 128, 256,$  and  $512$ . Plotted in the inset are the mean-square saturated width, calculated from the primary plotted data, against the size of the system on a double logarithmic scale.

#### IV. RESULTS FOR NONEQUILIBRIUM GROWTH

The nonequilibrium RSOS model is known to be described by the KPZ equation, given in Eq. (1). The critical exponents regarding the growth on a  $d$ -dimensional substrate were conjectured to be  $\beta = \frac{1}{d+2}$ ,  $\zeta = \frac{2}{d+3}$ , and  $z = 2\frac{d+2}{d+3}$  [11]. In regards to a fractal substrate, the question is posed whether or not the results obtained by substituting the substrate dimension by the fractal dimension agree with the numerical data. A previous study by Lee *et al.* indicated that the critical exponents were influenced by the detailed structure of the substrate [25]. In the followings, it will be shown that neither of these is correct with respect to the growth on a random fractal such as a percolation network.

Simulations are carried out first on pure square and simple cubic lattices, for comparison purposes. The growth and roughness exponents estimated are, respectively,  $\beta = 0.239(1)$  and  $\zeta = 0.390(1)$  in 2D, and  $\beta = 0.176(1)$  and  $\zeta = 0.307(2)$  in 3D. These values are smaller, by less than 10%, than the conjectured values. Since it is beyond the purpose of the present study to argue why the differences occurred, we here focus on the surface growth on a substrate with diluted sites.

In order to observe the influence of diluted sites on the critical exponents with respect to the nonequilibrium RSOS growth, simulations are conducted, regarding the cases of  $x=0.35$  in 2D and  $x=0.6$  in 3D. Figure 7 illustrates the data for  $W^2$  on a percolation cluster of the linear sizes  $L=32, 64, 128, 256,$  and  $512$  for  $x=0.35$  in 2D, and Fig. 8 represents those on a 3D cluster of the sizes  $L=8, 16, 32, 64,$  and  $128$  for  $x=0.6$ . For smaller size systems, data appear to follow the power-law behavior; however, as the system size increases, data deviate significantly from the power law, indicating that growth with respect to the nonequilibrium RSOS model displays nonuniversal behavior in both 2D and 3D. [It should be noted that the surface width in 3D exhibits a log-

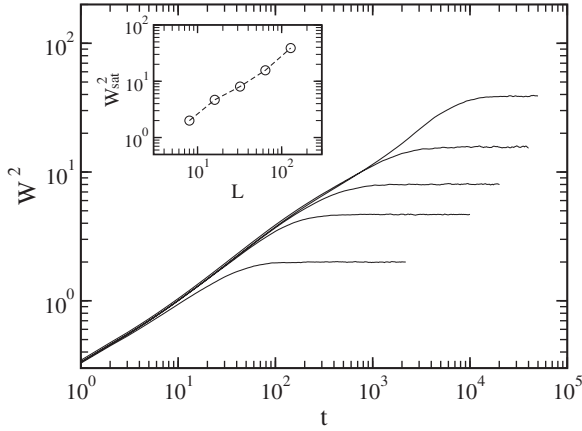


FIG. 8. The mean-square surface width  $W^2(L, t)$  for the nonequilibrium RSOS model on a 3D infinite percolation cluster for  $x = 0.6$ , plotted against the evolution time  $t$  on a double logarithmic scale. Data are for, from bottom to top,  $L = 8, 16, 32, 64,$  and  $128$ . Plotted in the inset are the mean-square saturated width, calculated from the primary plotted data, against the size of the system on a double logarithmic scale.

periodic oscillatory behavior in time.] Results for the saturated width also yield similar behaviors, as shown in the insets of both figures. These observations are a bit surprising because the percolation cluster is Euclidean for  $x < x_c$  and growth on such a Euclidean substrate is expected to be similar to that on a pure substrate, as observed with respect to the equilibrium growth. Such a nonuniversal behavior is rather similar to the behavior observed in absorbing phase transitions of the epidemic spreading, in which the quenched disorder yielded nonuniversal power-law behaviors in the Griffith phase [31,32]. The cause of a nonuniversal behavior is investigated in Sec. V.

Results for  $x = x_c$  are basically similar to those of  $x < x_c$ , but the nonuniversal behavior is more pronounced, as shown in Fig. 9 in 2D. The results in 3D are also similar to those of 2D (not shown).

Plotted in Fig. 10 are the data for  $W_{\text{sat}}^2$  regarding various size systems for the selected values of  $x$ , from bottom to top,  $x = 0, 0.1, 0.2, 0.3, 0.35,$  and  $x_c$  in 2D (left), and  $x = 0, 0.2, 0.5, 0.6,$  and  $x_c$  in 3D (right). In regards to  $x$  in close proximity to 0, the data show linear behaviors; however, as the value of  $x$  increases, e.g., for  $x = 0.2$  in 2D and for  $x = 0.5$  in 3D, the data exhibit a slight curvature, indicating that the data do not follow a power-law behavior. Therefore, the diluted sites influence the surface roughening in such a way as that the critical behavior is nonuniversal with respect to the nonequilibrium RSOS growth.

### V. SOURCE OF NONUNIVERSAL BEHAVIORS

A possible source of the nonuniversal behaviors might be either the influence of dangling ends of a percolation network, or the inhomogeneity of the substrates. In order to examine the former possibility, simulations are carried out on a 2D percolation network, with all dangling bonds eliminated, i.e., on a backbone network. In the equilibrium

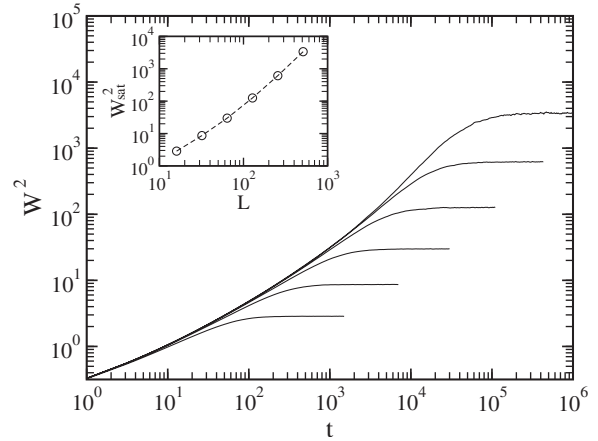


FIG. 9. The mean-square surface width  $W^2(L, t)$  for the nonequilibrium RSOS model on a 3D infinite percolation cluster for  $x = x_c$ , plotted against the evolution time  $t$  on a double logarithmic scale. Data are for, from bottom to top,  $L = 16, 32, 64, 128, 256,$  and  $512$ . Plotted in the inset are the mean-square saturated width, calculated from the primary plotted data, against the size of the system on a double logarithmic scale.

growth, the surface width and the saturated width exhibit power-law behaviors, with the exponents  $\beta = 0.185(3)$  and  $\zeta = 0.490(2)$ , which are in perfect harmony with the values predicted by Eq. (6),  $\beta = 0.186$  and  $\zeta = 0.485$ , having been obtained using  $d_f^{bb} \approx 1.64$  [48,49] and  $d_w^{bb} \approx 2.61$  [39]. In the nonequilibrium growth, neither the surface width nor the saturated width exhibit power-law behaviors, indicating that the growth behavior is nonuniversal on a percolation backbone (not shown). This observation rules out the former possibility.

In order to examine the latter possibility, simulations are conducted for the growths on substrates diluted by two different methods. The given  $L \times L$  system is divided into a number of  $l \times l$  subcells. In each subcell, 25% of the lattice sites are diluted first regularly and second randomly. It is

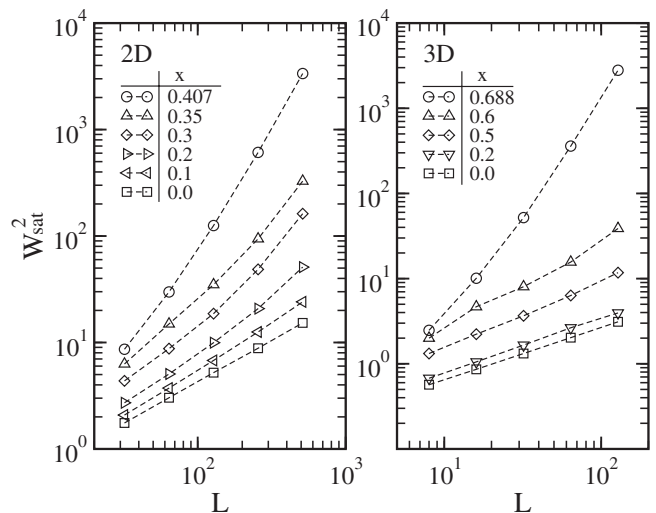


FIG. 10. The mean-square surface width  $W_{\text{sat}}^2$  against the size of system  $L$ , plotted on a double logarithmic scale, for selected values of  $x$  in 2D (left) and in 3D (right).

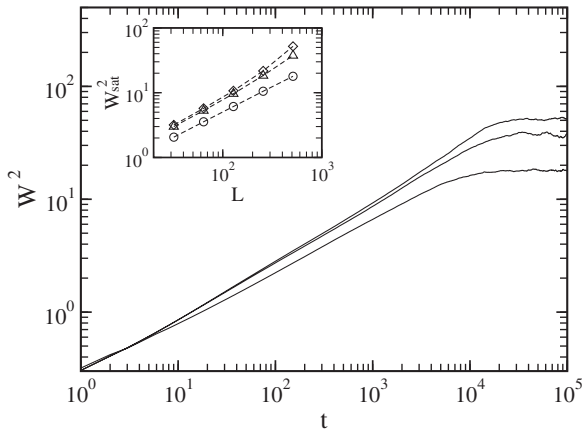


FIG. 11. The mean-square surface width  $W^2(L, t)$  against the evolution time  $t$ , for the nonequilibrium RSOS model on a substrate constructed with regularly diluted subcells (bottom) as well as randomly diluted subcells of two different sizes,  $l=8$  (middle) and  $l=16$  (top), both for  $L=512$ . A total of 25% of the lattice sites are diluted in each subcell. The inset shows data for  $W_{\text{sat}}^2(L)$  for the three cases.

determined that both the surface width and the saturated width with respect to the nonequilibrium RSOS growth on a substrate constructed with regularly diluted subcells yield power-law behaviors, with the exponents  $\beta=0.233(1)$  and  $\zeta=0.391(1)$ , which are very close to the values of a regular lattice presented earlier. This observation is precisely as predicted because the substrate is Euclidean and the critical exponents for the growth are similar to those of a regular lattice.

In regards to the growth on a substrate constructed with randomly diluted subcells, on the other hand, the results are different. Figure 11 shows the mean-square surface width for the systems of  $L=512$  constructed with subcells of two different sizes,  $l=8$  and  $16$ , in comparison with the data for the regularly diluted substrate. The plots in the inset represent the saturated widths. It is clear that data for the regularly diluted subcells exhibit power-law behaviors for both the surface width and the saturated width. However, regarding the randomly diluted subcells, data exhibited curvatures, indicating that the power-law characteristic is no longer valid; the larger the subcell is, the more pronounced the curvature is. It should be noted that if the size of a subcell is the same as the size of the system, the results would be the same as those on a percolation cluster for  $x=0.25$ . Thus, it is clear that the source of nonuniversal behavior involves the random dilution of lattice sites. The random dilution creates various sizes of diluted holes on a substrate, which destroy homogeneity and the translational invariance of the substrate, also possibly causing the nonuniversal behavior with respect to the nonequilibrium growth.

## VI. SUMMARY AND CONCLUSIONS

The influence of diluted sites on the growth has been studied for the equilibrium and nonequilibrium RSOS models. It

was found that, with respect to the equilibrium growth, both the surface width and the saturated width exhibited universal power-law behaviors for all cases regarding the concentration of diluted sites  $x$ . For  $x < x_c$ , the growth appeared to be similar to that on a regular lattice both in 2D and 3D. This observation had been expected because, for  $x < x_c$ , the substrate is Euclidean and the growth on such a Euclidean lattice is similar to that on a regular lattice. For  $x = x_c$ , on the other hand, the substrate becomes fractal and the growth yielded nontrivial exponents that were different from those on regular lattices.

In the nonequilibrium growth, on the other hand, a considerable amount of disorder  $x \leq x_c$  yielded nontrivial effects on the growth, and the growth became nonuniversal; both the surface width against the evolution time and the saturated width against the size of system did not follow the power-law behaviors, unlike the case for the equilibrium growth. Similar nonuniversal behavior was previously observed in absorbing phase transitions of the contact process, in which the quenched disorder yielded nonuniversal power-law behaviors regarding the density of active particles in the Griffith phase. The “quenched disorder” in this problem implies the dilution of lattice sites. Considering both this and the observations regarding the surface growth, it is conjectured that the quenched disorder might yield nonuniversal critical behaviors with respect to the nonequilibrium systems.

The cause of nonuniversal growth dynamics had been investigated, by considering the growth on a backbone network and on substrates constructed with periodically and randomly diluted subcells. It was found that the growth on a periodically diluted lattice yielded universal power-law behaviors, with the critical exponents being consistent with those on a regular lattice; however, the growth on a backbone and on a substrate with randomly diluted subcells were found to yield nonuniversal behaviors. Based on these results, it is clear that the random dilution of lattice sites is the main cause of such nonuniversal behaviors. The random dilution of lattice sites creates various sizes of diluted holes on a substrate, which subsequently destroy homogeneity and the translational invariance of the substrate. Such inhomogeneity appears to cause the nonuniversal behavior with respect to the nonequilibrium growth. In regards to the equilibrium growth, on the other hand, such behaviors appeared to cancel each other precisely during the processes of deposition and evaporation, and the resulting behaviors appeared to be universal.

## ACKNOWLEDGMENTS

This work was supported by the Korea Research Foundation Grant, funded by the Korean Government (Grant No. KRF-2008-313-C00329), and also in part by the Korea Science and Engineering Foundation (Grant No. 2009-0058988). The authors are grateful for the support.

- [1] F. Family and T. Vicsek, *Dynamics of Fractal Surfaces* (World Scientific, Singapore, 1991).
- [2] A.-L. Barabási and H. E. Stanley, *Fractal Concepts in Surface Growth* (Cambridge University Press, Cambridge, England, 1995).
- [3] D. A. Huse and C. L. Henley, Phys. Rev. Lett. **54**, 2708 (1985).
- [4] J. M. Burgers, *The Nonlinear Diffusion Equation* (Reidel, Boston, 1974).
- [5] M. J. Vold, J. Colloid Sci. **14**, 168 (1959).
- [6] M. Kardar and Y.-C. Zhang, Phys. Rev. Lett. **58**, 2087 (1987).
- [7] J. M. Kim, M. A. Moore, and A. J. Bray, Phys. Rev. A **44**, 2345 (1991).
- [8] M. Kardar, G. Parisi, and Y.-C. Zhang, Phys. Rev. Lett. **56**, 889 (1986).
- [9] R. Jullien and R. Botet, Phys. Rev. Lett. **54**, 2055 (1985).
- [10] P. Meakin, P. Ramanlal, L. M. Sander, and R. C. Ball, Phys. Rev. A **34**, 5091 (1986).
- [11] J. M. Kim and J. M. Kosterlitz, Phys. Rev. Lett. **62**, 2289 (1989).
- [12] S. F. Edwards and D. R. Wilkinson, Proc. R. Soc. London, Ser. A **381**, 17 (1982).
- [13] C. Herring, J. Appl. Phys. **21**, 301 (1950); W. W. Mullins, *ibid.* **28**, 333 (1957).
- [14] F. Family and T. Vicsek, J. Phys. A **18**, L75 (1985).
- [15] B. M. Forrest and L.-H. Tang, Phys. Rev. Lett. **64**, 1405 (1990).
- [16] J. G. Amar and F. Family, Phys. Rev. A **41**, 3399 (1990).
- [17] V. G. Miranda and F. D. A. Aarão Reis, Phys. Rev. E **77**, 031134 (2008).
- [18] T. Halpin-Healy and Y.-C. Zhang, Phys. Rep. **254**, 215 (1995).
- [19] L.-H. Tang and H. Leschhorn, Phys. Rev. A **45**, R8309 (1992).
- [20] S. V. Buldyrev, A.-L. Barabási, F. Caserta, S. Havlin, H. E. Stanley, and T. Vicsek, Phys. Rev. A **45**, R8313 (1992).
- [21] C. Lee and J. M. Kim, Phys. Rev. E **73**, 016140 (2006).
- [22] H. S. Song and J. M. Kim, J. Korean Phys. Soc. **53**, 1802 (2008); **51**, 1630 (2007).
- [23] G. Poupard and G. Zumofen, Phys. Rev. E **50**, R663 (1994).
- [24] T. Matsuyama and K. Honda, J. Phys. Soc. Jpn. **66**, 2533 (1997).
- [25] S. B. Lee, H.-C. Jeong, and J. M. Kim, J. Stat. Mech.: Theory Exp. 2008, P12013.
- [26] G. Zumofen, J. Klafter, and A. Blumen, Phys. Rev. A **45**, 8977 (1992).
- [27] S. B. Lee and J. M. Kim, Phys. Rev. E **80**, 021101 (2009).
- [28] B. K. Chakrabarti and J. Kertész, Z. Phys. B: Condens. Matter **44**, 221 (1981); K. Barat and B. K. Chakrabarti, Phys. Rep. **258**, 377 (1995).
- [29] K. Kremer, Z. Phys. B: Condens. Matter **45**, 149 (1981).
- [30] S. B. Lee and H. Nakanishi, Phys. Rev. Lett. **61**, 2022 (1988).
- [31] A. G. Moreira and R. Dickman, Phys. Rev. E **54**, R3090 (1996).
- [32] R. Dickman and A. G. Moreira, Phys. Rev. E **57**, 1263 (1998).
- [33] A. B. Harris, J. Phys. C **7**, 1671 (1974).
- [34] P. G. de Gennes, *Scaling Concepts in Polymer Physics* (Cornell University Press, Ithaca, New York, 1979).
- [35] M. P. M. den Nijs, J. Phys. A **12**, 1857 (1979).
- [36] B. Nienhuis, J. Phys. A **15**, 199 (1982).
- [37] P. N. Strenski, R. M. Bradley, and J. M. Debierre, Phys. Rev. Lett. **66**, 1330 (1991).
- [38] S. Alexander and R. Orbach, J. Phys. (Paris), Lett. **43**, 625 (1982).
- [39] S. Havlin and D. Ben-Avraham, Adv. Phys. **51**, 187 (2002).
- [40] R. M. Ziff and B. Sapoval, J. Phys. A **19**, L1169 (1986) and references therein.
- [41] M. E. J. Newman and R. M. Ziff, Phys. Rev. Lett. **85**, 4104 (2000).
- [42] X. Feng, Y. Deng, and H. W. J. Blöte, Phys. Rev. E **78**, 031136 (2008).
- [43] H. G. Ballesteros, L. A. Fernández, V. Martín-Mayor, A. Muñoz Sudepe, G. Parisi, and J. J. Ruiz-Lorenzo, J. Phys. A **32**, 1 (1999).
- [44] J. Hoshen and R. Kopelman, Phys. Rev. B **14**, 3438 (1976).
- [45] C. Vanderzande and A. Komoda, Phys. Rev. A **45**, R5335 (1992).
- [46] M. D. Rintoul, J. Moon, and H. Nakanishi, Phys. Rev. E **49**, 2790 (1994).
- [47] S. B. Lee, Int. J. Mod. Phys. B **17**, 4867 (2003).
- [48] M. D. Rintoul and H. Nakanishi, J. Phys. A **25**, L945 (1992).
- [49] P. Grassberger, J. Phys. A **25**, 5475 (1992).